Soil Dynamics and Earthquake Engineering 124 (2019) 86–97

Contents lists available at ScienceDirect

Soil Dynamics and Earthquake Engineering

journal homepage: www.elsevier.com/locate/soildyn

Nonlinear dynamic analysis of frame-core tube building under seismic sequential ground motions by a supercomputer

Jiaxu Shen[a], Xiaodan Ren[a], Yongqun Zhang[b], Jun Chen[a,c,*]

[a] Department of Structural Engineering, College of Civil Engineering, Tongji University, Shanghai, PR China
[b] Shanghai Key Laboratory of Engineering Structure Safety, Shanghai Research Institute of Building Sciences, Shanghai, PR China
[c] State Key Laboratory of Disaster Reduction in Civil Engineering, Tongji University, Shanghai, PR China

ARTICLE INFO

Keywords:
Sequential ground motions
Core tube structure
Supercomputer
Nonlinear dynamic analysis

ABSTRACT

Historical records indicate that strong earthquakes are usually accompanied by aftershocks with large peak ground accelerations. Structural damages caused by the mainshock can be further aggravated by aftershocks, which can lead to structural collapse. Current structure seismic design practices generally consider the mainshock effects only. Performance of buildings subjected to mainshock-aftershock sequential ground motions, should always be fully investigated. Previous studies on sequential ground motion focus mainly on frame structures. There is a paucity of publications addressing other type of structures, especially high-rise buildings. The reasons for this omission have been identified as the complexity of high-rise buildings and unaffordable computational costs related to the nonlinear dynamic analysis of long duration sequential ground motions. Thus, the authors used Tianhe-2, once known as the fastest supercomputer in the world, to conduct nonlinear dynamic analysis of a typical 20-story frame-core tube building subjected to sequential mainshock-aftershock ground motions. This study focuses on 104 mainshock and aftershock ground motions from four different sites. Thus, the effects of mainshocks only and sequential ground motions of a frame-core tube structure at four different sites were analyzed in this study's finite element model. The Performance of these structures under mainshocks and sequential ground motions are compared in terms of inter-story displacement ratio, hysteretic energy and damage index based on the Park-Ang model. The results prove that a supercomputer can be used to solve the computational cost issue in structural engineering and emphasize that the effects of sequential earthquakes need to be considered in structural design, even for frame-core tube structures with lateral resisting members.

1. Introduction

Earthquakes are one of the most serious disasters that endanger the safety of people's lives and properties. The mainshock and aftershocks forms sequential ground motions. In recent years, sequential mainshock-aftershock seismic activity has caused tremendous losses to society. The compounding effect of the damage and disruption caused by earthquake sequential ground motion reactions have made seismic history in Chi-Chi (1999) [1], Wenchuan (2008) [2], Christchurch (2010–2011) [3], Tohoku (2011) [4], and Nepal (2015) [5]. These are just a few examples of major earthquakes that have caused tremendous human loss and cost. Based on a 2012 report by the Center for Disaster Management and Risk Reduction (CEDIM) in Germany, in 2011 alone, worldwide seismic loss included 133 earthquakes (including aftershocks) and their consequences (i.e., tsunamis, landslides, ground settlements) caused $365 billion worth of damage including the death of 20,500 people and the loss of homes to approximately one million people. CEDIM shared the assessment of the Tohoku earthquake damage, where the tremendous loss from the Tohoku earthquake was said to be mostly due to “aftershocks” [6].

Therefore, understanding the sequential ground motions and the response of the structure subjected to sequential ground motions in perspective is of great significance to the improvement of planning for seismic events and the development of post-earthquake emergency responses and recovery strategies.

The study of sequential ground motions dates back to 1894 when Omori [7] summarized the law of frequency attenuation of aftershock with time. After more than 100 years of exploration, the research on sequence earthquakes has achieved fruitful results, including the famous Gutenberg-Richter law [8] and Bath law [9]. In 1980, Mahin's seminal work [10] made a breakthrough by connecting sequential ground motions with structures, changing the post-seismic ground

* Corresponding author. Department of Structural Engineering, College of Civil Engineering, Tongji University, Shanghai, PR China.
E-mail address: cejchen@tongji.edu.cn (J. Chen).

https://doi.org/10.1016/j.soildyn.2019.05.036
Received 12 March 2019; Received in revised form 22 May 2019; Accepted 22 May 2019
Available online 30 May 2019
0267-7261/

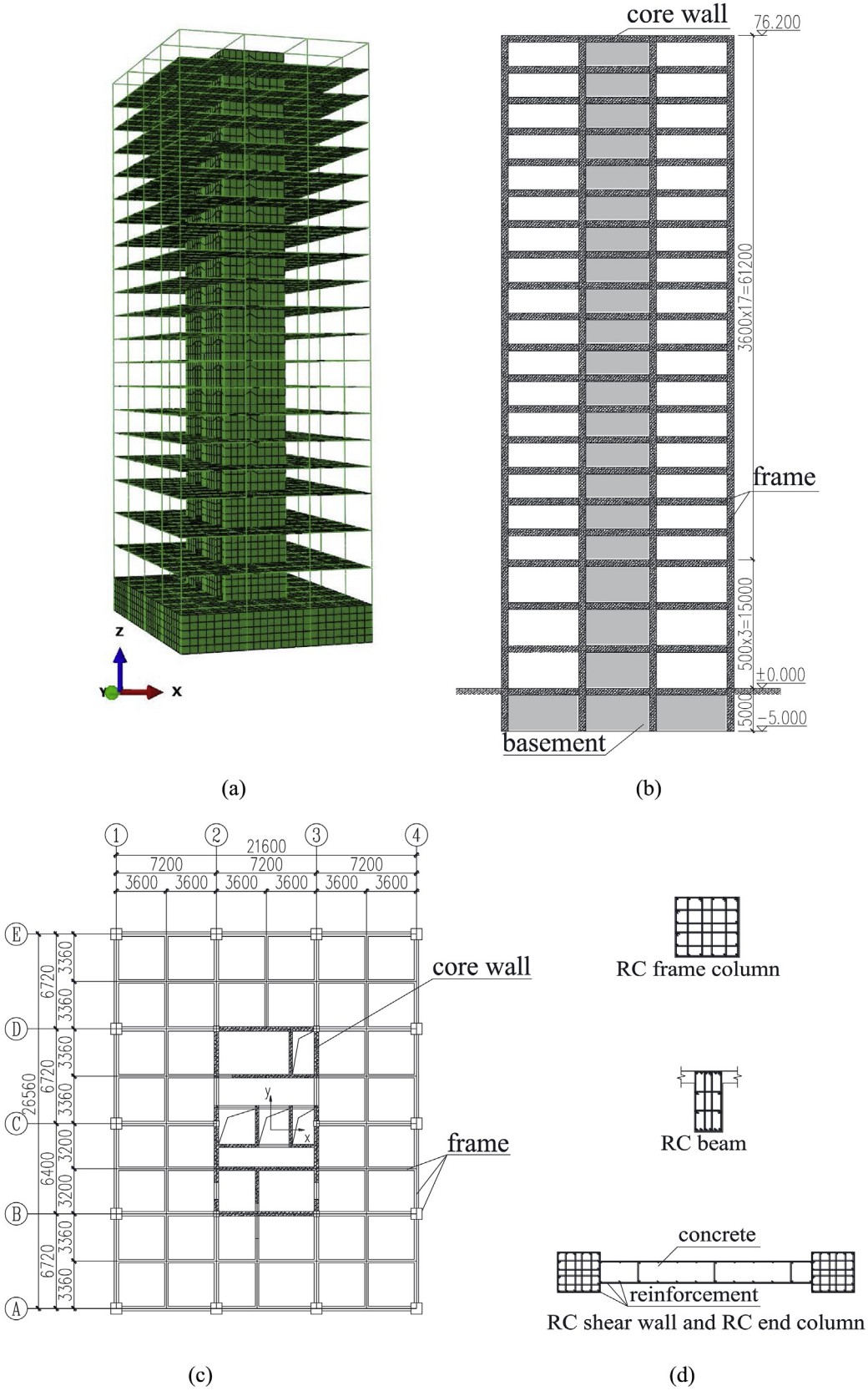

Fig. 1. (a) Finite element model, (b) Vertical section of frame-core tube structure, (c) Layout, and (d) Partial members.

Table 1
Material properties.

Material	Grade	Elastic modulus	Tensile strength	Compressive strength	Part
Concrete	C40	32.5 GPa	3.2 MPa	36 MPa	Beam, Floor
Concrete	C50	34.5 GPa	3.5 MPa	42 MPa	Column, Wall
Bar	HRB400	200 GPa	400 MPa	400 MPa	

motions from a concept in the field of seismology, to a major research direction in earthquake engineering. Since then, scholars have begun to study sequential ground motions from different perspectives. In the early single degree of freedom (SDOF) system studies, two research routes were developed: 1) the SDOF system or the equivalent SDOF system, which focuses mostly on frame structure and 2) for complex structures such as long-span bridges [11], a refined numerical method was often used.

Under the first frame-structure focused SDOF system method, several as-recorded and artificially generated ground motions were applied to the SDOF system to obtain an inelastic response spectrum, such as the damage spectrum [12] and strength reduction factor spectrum [13]. Other researchers focused on the response of frame structures subjected to sequential ground motions. The structural vulnerability curve was obtained by Monte Carlo simulation or incremental dynamic analysis (IDA) [14–16]. Based on these studies, the inelastic response spectrum and vulnerability curve were obtained as important evidence to guide engineering design and verification.

In the second numerical method, the study of complex structures Ruiz-García et al. [11] analyzed 28 mainshock-aftershock seismic sequences of highway bridges based on records from sites near the subduction zone of the Mexican Pacific coast. They noted several RFC piers of a nine-span freeway overpass bridge were damaged in the 1987 Whittier Narrows earthquake (Mw = 5.9) three days after mainshock seismic activity. Thus, aftershocks were shown to cause additional damage. Despite the sophistication of current research modeling procedures, aftershock seismic analysis is still in the verification stage in many cases. Thus, seismic performance of complex structure responses based on post-earthquake file reconnaissance of aftershock ground motions is still in need of more attention and development.

In the first method, studies of complex structures and their equivalent SDOF system are studied separately for two reasons. The first reason is that the equivalent SDOF system is widely researched under mainshock conditions and extensively applied in construction. The research route is very clear. The other reason is the difficulty in calculating complex structures because of limitations in computational power. The complexity of structure combined with the long-term characteristics of sequential ground motions bring great challenges to computing devices. The huge amount of calculations and unbearable time costs have hindered the development of seismic performance analysis of complex structures under sequential ground motions.

With the development of urban construction, the number of high-rise and super-tall buildings with various structural forms is increasing rapidly. By the end of 2018, 144 super-tall buildings extended upward by as much as 300 m worldwide, and more than 1400 buildings were over 200 m in height [17]. The construction of high-rise and super-tall buildings has greatly improved the functionality of cities. The accompanying structural safety issues, however, cannot be ignored. Although the general high-rise building can exhibit good resistance to a mainshock due to the setting of the shear members, limited knowledge has been published on the response and performance of high-rise buildings in the case of sequential ground motion. Moreover, current research shows that, in sequential ground motions, significant differences have been found between the spectral characteristics of the mainshock and aftershocks. In addition, artificial seismic sequences lead to an overestimation of maximum lateral drift demands compared with the response of structures subjected to as-recorded seismic sequences [18]. Another question to be studied is which evaluation index should be chosen to effectively assess the structural damage. In the evaluation of the equivalent SDOF system, the scholars used the dissipated energy, the inter-layer displacement ratio or the Park-Ang damage index to evaluate the structural damage [19,20]. For high-rise buildings, which index is more suitable is still to be investigated. Therefore, if only a few sequences are selected for analysis, it is difficult to draw a solid conclusion. The use of a more reliable analysis method is urgently needed for high-rise buildings subjected to mainshock-aftershock seismic sequences so as to more systematically evaluate their structural performance level and protect the structure itself as well as the safety of human life and property.

In this paper, a high-rise building's typical structural form, the frame-core tube is the primary research focus. The authors collected 104 as-recorded sequential seismic ground motions from four different site classes. The response and performance level of the frame-core tube structure subjected to sequential ground motion are presented in this study. The authors' aim is to break through the limitation of traditional complex structure analysis methods by using more scientific evaluation indicators and research methods, to gain a deeper understanding of the responses and performance levels of frame-core tube structures under sequential seismic ground motions.

2. Establishment of finite element model of tall building

This paper presents an existing 20-stories, 81.2 m-tall, frame-core tube structure, as shown in Fig. 1. The cross section of the frame column measures 900 mm × 900 mm. The frame beam cross section is 400 mm × 800 mm. The thickness of the outer shear wall is 400 mm. The inner shear wall of the core tube 250 mm. The thickness of each floor is 120 mm. The material properties of each component in the structure are shown in Table 1.

As shown in Fig. 1 (a), a finite element model with a total of 39,291 regular elements, including 21,673 shell elements and 17,618 beam elements is established. For the constitutive laws, the kinematic hardening of model steel and the plasticity model of concrete with damage energy consumption have been considered. Mass-proportional Rayleigh damping model is adopted. In addition, to more realistically simulate the nonlinear performance of the structure, the beam and column use fiber beam elements, and the floor and shear wall use a multilayer shell element [21–23].

The fiber beam element model is the most commonly used model in finite element simulation of beams and columns in a frame [24,25] because it provides a good balance between accuracy and computational efficiency. As shown in Fig. 2, the beam and column are discretized into beam elements with multiple integration points based on the displacement formula or force formula. At each integration point, the relationship between forces (e.g., bending moment and axial force) and deformations (e.g., curvature and axial strain) is imposed. To consider the interaction between the nonlinear beam-column bending moment and the axial force, the section corresponding to the integration point is divided into fibers, and a uniaxial stress-strain relationship can be applied to the fiber. According to the Euler–Bernoulli hypothesis, the strain of each fiber over the section can be determined based on section deformations, including the curvature and axial strain. In the meanwhile, internal forces, such as the bending moments and axial forces, can be determined by integrating the fiber stresses in the section.

The multilayer shell element [26] was originally developed for the simulation of composite materials. Fig. 3 shows a shell element in the model divided into several layers. Then, the thickness and material properties (concrete or steel) of the layers are appointed based on the actual conditions of the shear wall. When calculating with the finite element method, the strain and curvature of the central layer of the shell elements are obtained first. According to plane section assumption, the strain of each concrete layer and the steel layer can be derived

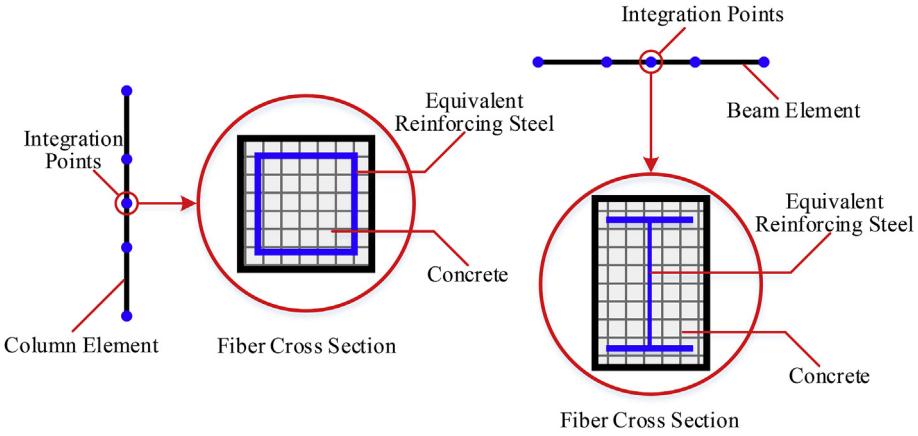

Fig. 2. Fiber beam element.

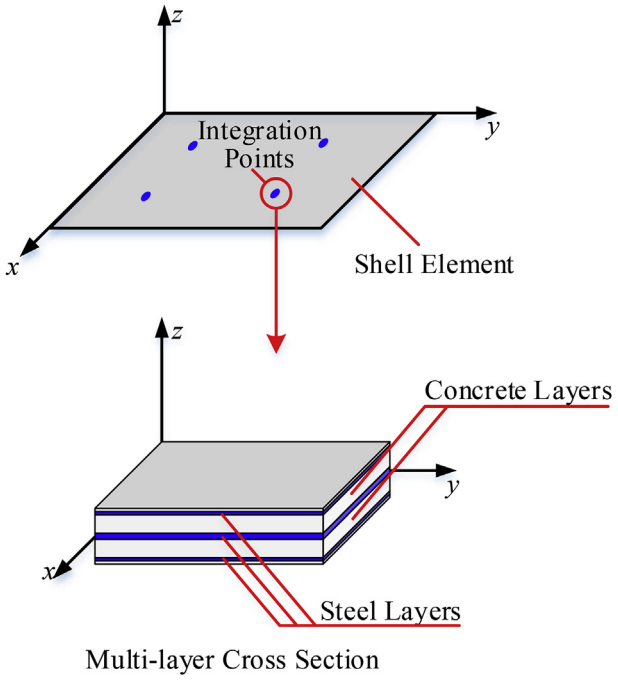

Fig. 3. Multilayer shell element.

from the strain and curvature of the central layer. The corresponding stress is obtained from the constitutive equation of each material. Eventually, the internal force of the entire shell element can be obtained through integration. The multilayer shell element can more accurately simulate the complex nonlinear mechanical behavior of the actual shear wall.

3. Selection of sequential ground motions

Selection of earthquake ground motions is a presupposition for structural seismic response assessment. The artificially generated sequential seismic ground motion will overestimate the structural response [18]. In addition, due to the inherent random characteristics of ground motions, if the number of earthquakes selected for analysis is too limited, the reliability of the conclusion is difficult to guarantee. Therefore, selecting enough as-recorded sequential ground motions as load inputs is essential to the success of a project. In this paper, 104 two-sequence ground motion records were selected from the Pacific Earthquake Engineering Research Center (PEER) [27] and strong-motion seismograph networks (KiK-net, K-NET) [28].

Selection principles are as follows:

(1) To avoid soil-structure interaction effects, the seismograph stations which record the selected ground motions should be located on a free site or on the ground floor of low-rise buildings.
(2) The fault distance should be larger than 10 km to reduce the influence of near-field effect.
(3) All records should be from the same station and the same seismic event. The record with the earlier occurrence had a peak ground acceleration (PGA) greater than 0.10 g, which was taken as the main shock. The latter ground motion with the second largest PGA greater than 0.05 g was recorded as an aftershock.
(4) The magnitude of mainshocks and aftershocks should be larger than Mw 6.0 and Mw 5.0, respectively, excluding earthquakes that are unlikely to affect a structure.
(5) To ensure that the structure is at rest before the aftershocks and to consider the calculation time, a time interval of 100 s is added between the mainshock ground motion and the aftershock ground motion which we selected.
(6) To research the influence of the site class on the structural response and damage state, sequential ground motions should be classified according to the site category. According to the code for seismic design of buildings, the site category is divided into four classes based on a soil thickness of 20 m and 30 m and equivalent shear wave velocities. The dividing standard [29,30] is shown in Table 2.

Based on the selection principle, 104 actual sequential ground motions were selected from 7 earthquakes, including 20 for site Class A, 28 for site Class B, 36 for site Class C and 20 for site Class D, as shown in Table 3. Examples of them are illustrated in Fig. 4. To facilitate a comparative analysis, the PGA of sequential seismic ground motion records were scaled to an identical value. Since the high-rise and supertall buildings are mainly located in megalopolises, this paper focuses on the structural response of their high-rise buildings under severe earthquakes. The PGA of the ground motion is adjusted to a value with the 50-year exceedance probability of 2%–3%, namely, 0.4 g. On the one hand, a high-rise structure can fully enter into the plastic phase, so, we can further study the nonlinear performance of the structure. On the

Table 2
Site classification criteria.

Site Class	Average Shear Wave Velocity V_{20} (m/s)	Average Shear Wave Velocity V_{30} (m/s)
A	> 500	> 596
B	250–500	278–596
C	150–250	158–278
D	< 150	< 158

Table 3
Selected ground motion record of main aftershock sequence.

Earthquake event	Mainshock		Aftershock		Site			
	Time	Mw	Time	Mw	A	B	C	D
Wen Chuan	2008.05.12 14:28	7.9	2008.5.12 19:11	6.1		4	2	
Chi-Chi	1999.09.20 17:47	7.6	1999.9.20 17:57	5.9	4	6	10	2
New Zealand	2010.09.03 16:35	7.0	2011.2.21 23:51	6.2		4	12	
East Japan Earthquake	2011.03.11 14:46	9.0	2011.3.11 15:15	7.7	14	12	14	6
Coast of Niigata	2007.07.16 10:13	6.8	2007.07.16 15:37	5.8				4
Niigata-ken Chuetsu	2004.10.23 17:56	6.8	2004.10.23 18:03	6.3				6
Kumamoto	2016.04.14 21:26	6.2	2016.04.16 01:25	7.0	2	4		2
Summation					20	28	36	20

other hand, several ground motions have been recorded in recent years, the PGAs of which far exceed the acceleration of structural design considerations, with some approaching 1 g (such as the 2008 Wenchuan earthquake and the Mw 9 2011 Tohoku earthquake, which started in Japan). Therefore, it is also a realistic requirement for structural earthquake resistance to adjust the PGA to 0.4 g.

To study the response of a structure subjected to horizontal one-way ground motions, horizontal components of seismic sequential ground motions were selected and applied separately along the weak axis direction of the structural cross section to investigate the structural response under adverse conditions. Ground motions are directly applied to the structural foundation, soil-structure interaction has not been considered.

4. Application of Tianhe-2

As mentioned earlier, computational power limitations are a major constraint on the study of seismic sequential ground motions. This limitation is especially significant in the analysis of complex structures such as long-span bridges and high-rise buildings. In this paper, the central difference method is utilized for analysis, which is suitable for multi-processor parallel computing. This method ensures stable calculation, good convergence and high computational efficiency. Even so, when the frame-core tube model has a complicated form and a large number of elements, it is still difficult for a common computer to accomplish such a large amount of calculation.

The commercialization of supercomputers has brought a new solution to this dilemma. Supercomputers have the advantages of excellent

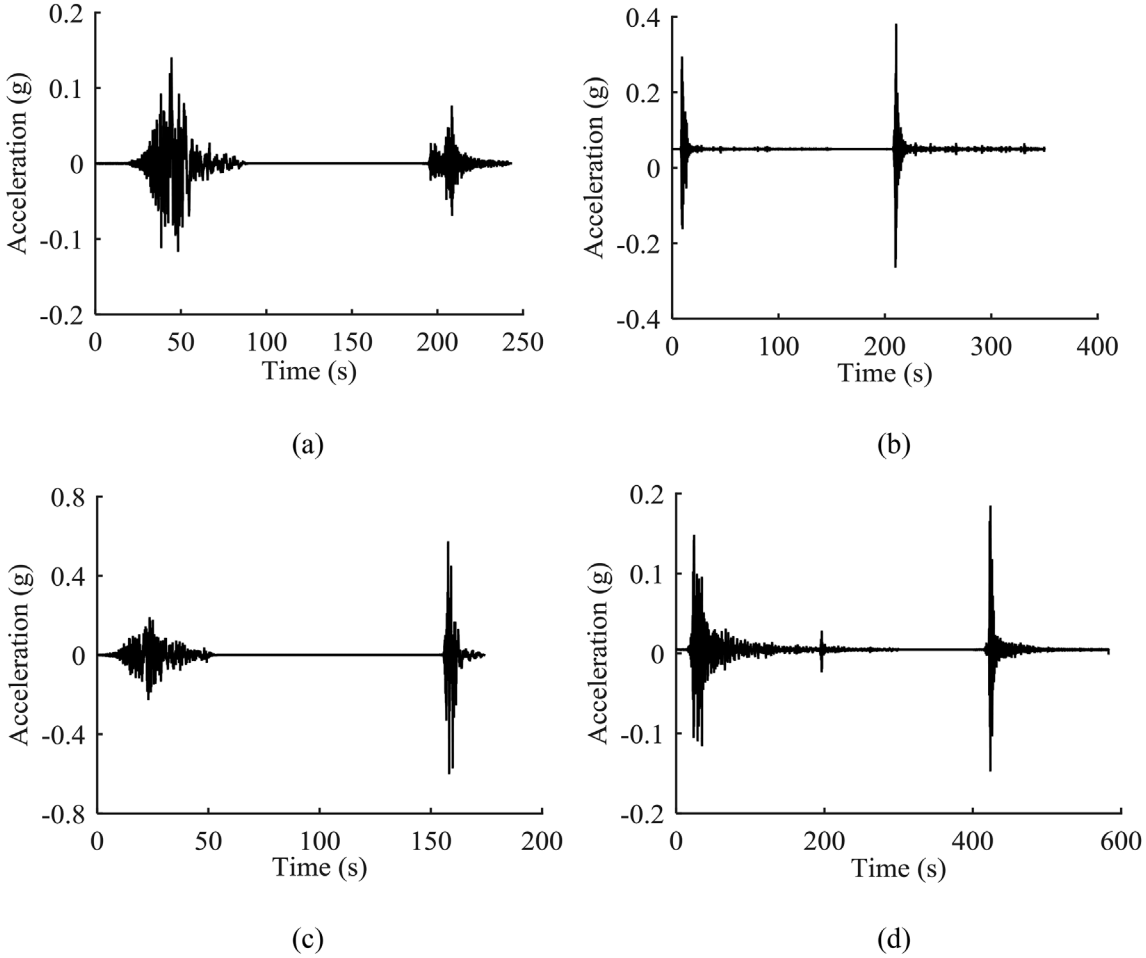

Fig. 4. Examples of sequential ground motions considered in this study: (a) TCU128EW (Chi-Chi, 1999.09.20), (b) KMMH16EW (Kumamoto, 2016.04.14), (c) Pages Road Pumping Station NS (Darfield-Christchurch, 2010.09.03), and (d) NIG013NS (Coast of Niigata, 2007.07.16).

Table 4
Comparison of calculation efficiency.

Computer	Unit calculation time	Calculate nodes	Total time
Tianhe	2d	40	6d
PC	8d	1	832d

computing power, submitting tasks in batches, processing data in batches, and producing reliable calculations. They have provided strong technical support for multiple subject areas, greatly improving computational efficiency and shortening computation time. Although supercomputers have been widely recognized and applied in meteorology, physics, life sciences, materials science and other fields, their application in structural engineering is still in its infancy.

The Tianhe-2 supercomputer platform is utilized in this research to realize batch parallel computing analysis of the core tube structure. Tianhe-2 was once the world's fastest supercomputer, which won six consecutive championships in a supercomputing conference [31]. Tianhe-2 has 16,000 compute nodes, each of which is equipped with two Xeon E5 CPUs and three Xeon Phi 57 accelerator cards. A total of 3.12 million computing cores are provided by 32,000 Xeon E5 CPUs and 48,000 accelerator cards. Its peak floating-point operation per second reaches 54,902.4 TFLOPS with a maximum computing power of 33,862.7 TFLOPS [32]. In contrast, the computing power of CPU (Intel i7-8700 K) commonly used in ordinary personal computers is only about 60 GFLOPS.

The calculation and analysis of the frame-core tube structure by means of the Tianhe-2 processor are realized by programing a batch program. Forty compute nodes are used, each of which computes a structural model subjected to a seismic sequential ground motion. For the calculation model established in this paper, Table 4 gives the comparison of the computational efficiency between Tianhe-2 and a personal computer. Clearly, the calculation efficiency of a single computing node is about 4 times that of a PC. The parallel processing using multiple nodes can increase efficiency to nearly 140 times of that of PC. It takes only 6 days to complete all calculations.

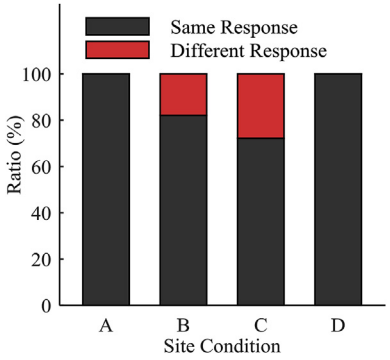

Fig. 6. Maximum displacement difference.

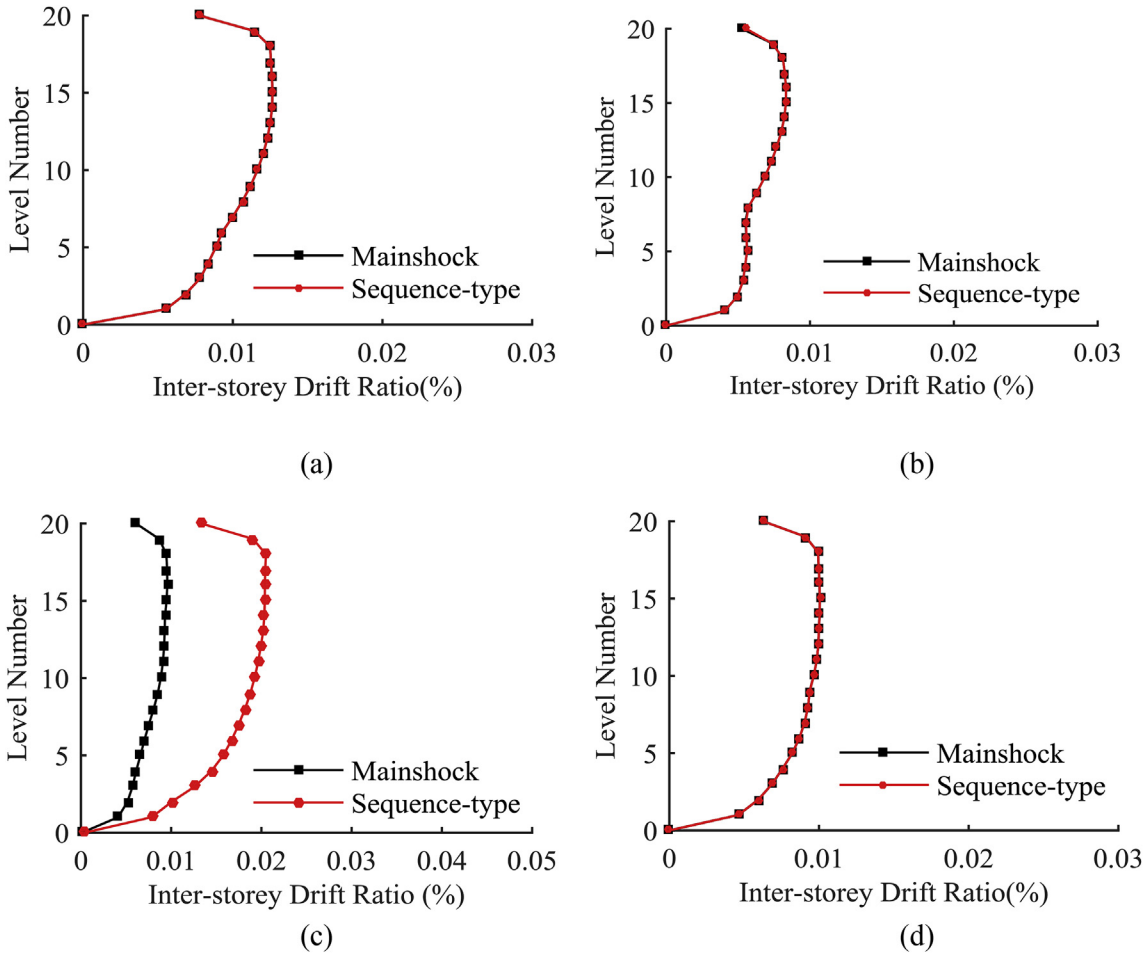

Fig. 5. Response (Inter-storey Drift Ratio) of the frame-core tube model under sequence-type ground motions: (a) TCU128EW (Chi-Chi, 1999.09.20), (b) KMMH16EW (Kumamoto, 2016.04.14), (c) Pages Road Pumping Station NS (Darfield-Christchurch, 2010.09.03), and (d) NIG013NS (Coast of Niigata, 2007.07.16).

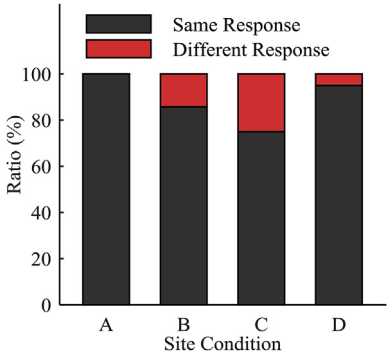

Fig. 7. Inter-story displacement ratio difference.

Table 5
Relationship between structural performance level and damage index.

Performance level	Slight	Minor	Moderate	Severe	Collapsed
Damage index (D)	< 0.1	0.1–0.25	0.25–0.4	0.4–1.0	> 1.0

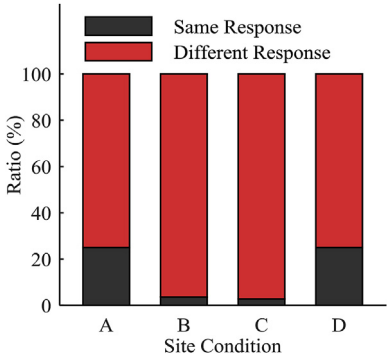

Fig. 8. Damage index differences.

5. Results and discussion

The amplitude, duration and spectral characteristics of the ground motions have a significant impact on the structural response. The ground motions' amplitudes were scaled to the same and a relatively large level (PGA = 0.4g) to study effects of other two factors without compromising amplitude's effect. The influence of duration on the structure is mainly reflected in the nonlinear phase of the structure, and its significance exists in both the first passage failure and the cumulative hysteresis energy of the nonlinear system. The maximum displacement, inter-story displacement ratio (IDR) and hysteretic energy in calculation results are investigated to study the effect of aftershocks on the frame-core tube structure. The response (IDR) of the frame-core tube model under examples in Fig. 4 is examined and shown in Fig. 5. Notably, some aftershocks, but not all aftershocks, can affect the displacement response of the structure. Based on this, the authors thoroughly investigated the displacement responses of the structure. The results are shown in Fig. 6 and Fig. 7. They show ratio of numbers of 'Same' cases and 'Different' cases over total number of selected records. The label means same or different values, e.g. maximum displacement or IDR, are obtained from mainshock-only input and sequential earthquakes input. Fig. 6 shows that very few seismic sequential ground motions can affect the maximum displacement of the frame-core tube structure (about 14%). In most cases, the aftershock only has a small effect on the maximum displacement of the structure. Fig. 7 compares the IDRs of the structure under mainshocks and seismic sequential ground motions. Obviously, the results are much like the ones of maximum displacement. More than 80% of the seismic sequential ground motions have the same effect on the IDR as the corresponding main shock. The aftershocks have less influence on the frame-core tube structure IDR, which is contrary to the reported effects of the 1995 Hyogoken-Nanbu (Kobe, Japan) earthquake by Chung [33]. This phenomenon compared favorably with Ruiz-Garcia's [18] 2011 report on the response of steel frames under actual sequence-type ground motions. Their conclusion was that aftershocks do not significantly increase the peak and residual displacement demands of existing steel frames. In addition, the reinforced concrete cylinder increases the rigidity of the structure, which causes less lateral displacement demand of the structure under horizontal ground motions compared with frame-type structure. Consequently, the displacement response doesn't increase significantly after aftershocks, but the hysteretic energy caused by shear force will increase. Therefore, it is not reasonable to rely solely on displacement as an index to measure the influence of aftershock on the frame-core tube structure. However, this does not fully reflect the cumulative damage effect of the structure subjected to seismic sequential ground motions.

Park et al. [34,35] proposed a two-parameter structural damage model considering the structure's first transcendence damage and cumulative damage effects, which has been widely used by scholars all over the world. It is a non-dimensional parameter to evaluate and describe the damage degree of components or structures under random earthquake excitations. The index is also an important basis for decision-making on the structure after earthquakes. In this paper, we consider the Park-Ang two-parameter damage model as the damage index needed to evaluate the damage degree of the structure. The model is

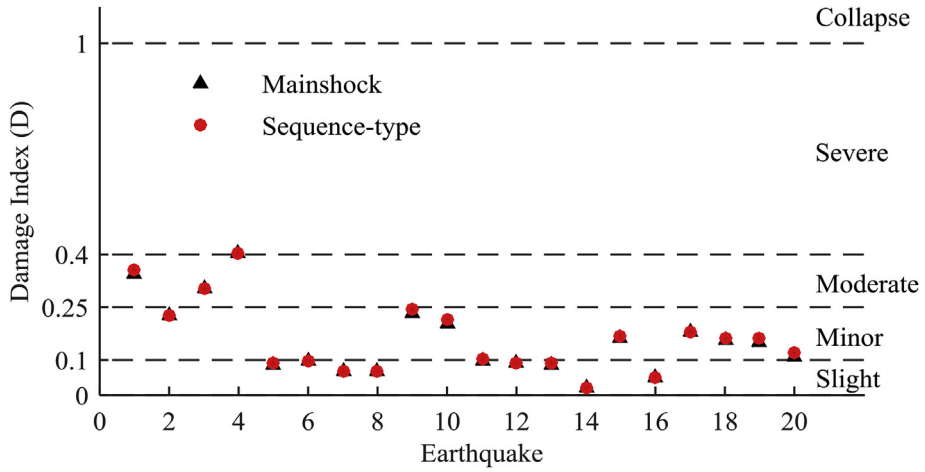

Fig. 9. Damage indexes on Site Class A.

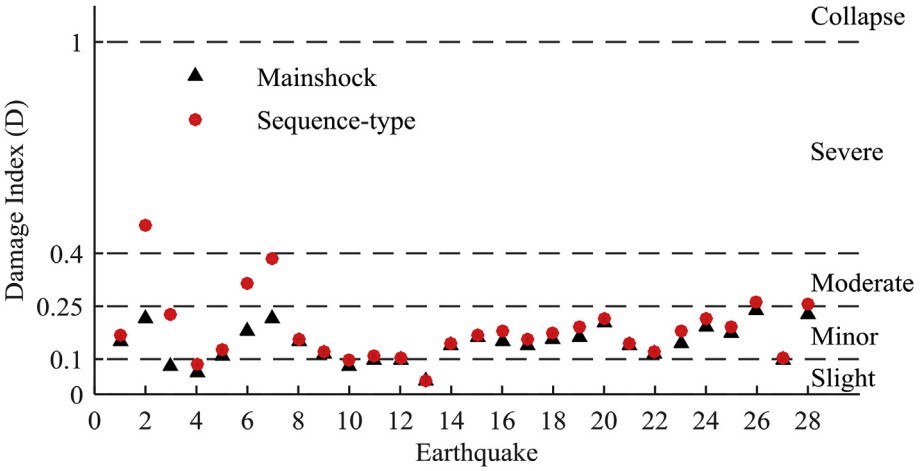

Fig. 10. Damage indexes on Site Class B.

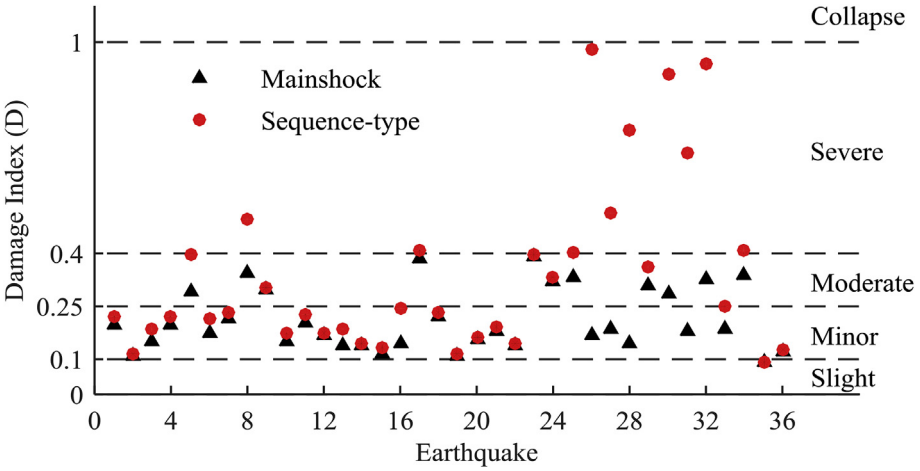

Fig. 11. Damage indexes on Site Class C.

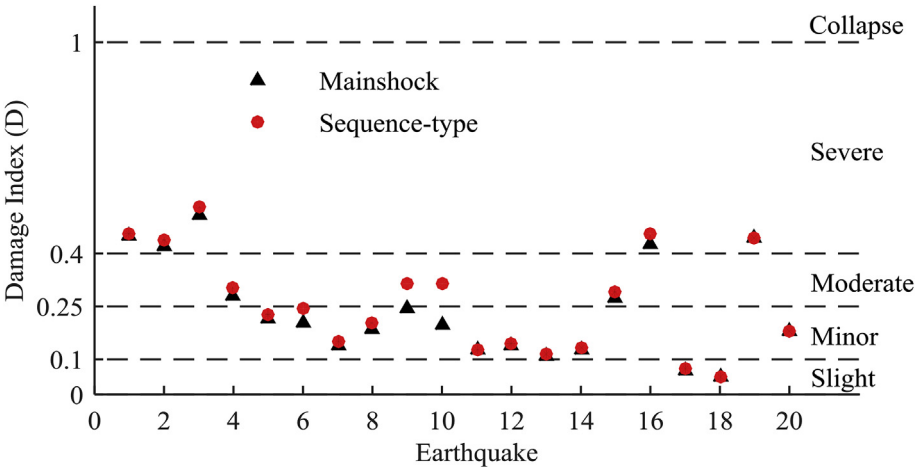

Fig. 12. Damage indexes on Site Class D.

obtained by linear superposition of the displacement term and an energy term, which can be expressed as:

$$D = \frac{x_m}{x_u} + \beta \frac{E_h}{F_y x_u}. \quad (1)$$

where x_m is the maximum response deformation, x_u is ultimate deformation capacity under static loading, E_h is cumulative hysteretic energy dissipation, F_y is calculated yield strength under static loading, and β is the energy dissipation factor, which can be calculated as follows:

$$\beta = (-0.447 + 0.073\lambda + 0.24n_0 + 0.314\rho_t) \times \rho_w \quad (2)$$

where λ is the shear span ratio (replaced by 1.7 if $\lambda \leq 1.7$), n_0 is the axial compression ratio (replaced by 0.2 if $n_0 \leq 0.2$), ρ_t is the

Table 6
Modal information of the structure.

Mode	Frequency (Hz)	Effective Mass (kg)		
		X	Y	Z
1	0.716	17334.0	82.0	0.0
2	0.750	74.2	18769.0	0.0
3	0.857	187.2	1.5	0.0
4	2.628	0.7	3227.8	0.1
5	2.825	292.2	22.9	0.3
6	3.051	3938.4	3.2	0.1
7	5.353	4.6	295.5	5.5
8	5.469	5.5	594.6	0.3
9	5.731	0.0	0.4	18118.0
10	6.211	0.2	65.4	21.1

longitudinal reinforcement ratio expressed as a percentage (replaced by 0.75% when $\rho_t \leq 0.75\%$), and ρ_w is the volume stirrup ratio expressed as a percentage.

The damage index of a single component is calculated based on Equation (1). By weighting and summing the damage index of individual components, the overall damage index of the structure can be obtained. The overall damage index can be expressed as:

$$D = \sum_{i}^{N} \lambda_i D_i \tag{3}$$

where D is the overall damage index of the structure, N is the number of structural components, D_i is the damage index of the i component, and λ_i is the weighting coefficient of the i component, which is calculated by the following formula:

$$\lambda_i = \frac{E_i}{\sum E_i}. \tag{4}$$

where E_i is the hysteretic energy of the i component.

Based on the indicators obtained by Park [35] and Kunnath [36], the seismic structural damage was mainly divided into five performance levels. The damage index range corresponding to each performance level is shown in Table 5.

As shown in Fig. 8, during the actual ground motion, the structure will be damaged after the mainshock. Due to the short time interval between the mainshock and aftershocks, the structure will undergo cumulative damage again after undergoing the aftershocks without repair. Therefore, the damage index of the structure after the sequence shock is almost greater than the damage index after only the mainshock; thus, the aftershocks increase the damage of the structure, which is consistent with the results of the earthquake damage investigation.

Since the concept of damage index contains a displacement term and a hysteretic energy dissipation term, the impact of the aftershock on the damage index is between the two terms. Figs. 9–12 show the damage index of the structure under the excitation of each ground motion in four different site classes. Thus, during the excitation of the mainshock, the structural damage index is almost less than 0.4. Only a few indexes of the site class D are larger than 0.4, accounting for about 5% of the total. $D = 0.4$ is the repairable and irreparable boundary proposed by the Park-Ang model [35]:

If $D \leq 0.4$, the structure is repairable;

If $D > 0.4$, the structure is difficult to repair;

If $D > 1.0$, the structure has collapsed.

Therefore, under the excitation of the main shock, the overall collapse or serious damage to the frame-core tube structure can be avoided. In addition, the damage is basically within the repairable range, and the safety of the structure can be guaranteed.

Under the excitation of seismic sequential ground motions, the structural damage index effects were different under the aftershocks recorded for various site classes. The aftershocks on site class A had only a minor effect on the structural damage indexes. Damage indexes increase by about 10% on average, which is not enough to change their performance level. The structure had only minor or moderate damage under seismic sequential ground motions. For site class B, structural damage indexes under the excitation of aftershocks increased to different extents, averaging out at about 27%. A few indexes will exceed their original level of performance, which results in more serious damage, which can also be unrepairable. Obviously, the aftershocks on site class C had a great impact on the structure. The structural damage indexes generally have a large increase, averaging out at about 67%. Some indexes are in a repairable state under the excitation of mainshock, but when suffering aftershocks, the indexes increase several times, up to 1.0, which indicates a state of near collapse. The influence of aftershocks on the site class D building is not significant. Structural damage indexes increase by about 11% on average. In the selected sequential ground motions from the site class D, no aftershock occurred that could change the structural performance level. Nevertheless, different from the other three site classes, a mainshock on site class D could cause serious damage to the structure, i.e., $D > 0.4$. Therefore, for the design of frame-core tube structure located on site classes B, C, and D, especially on site class C, the impact of aftershocks on the structure should be fully considered.

For those aftershocks causing severe structural damage, their spectral characteristics, besides amplitudes and durations, are explored as another factor.

First, the modal analysis of the frame-core tube structure was carried out to analyze its structural dynamic characteristics. The effective masses of the first 10 natural frequencies and the three translational directions are shown in Table 6.

The first three natural periods of the structure are longer, and the period is slightly larger than 1.0 s, which is likely to coincide with the predominant period of ground motions. In this research, seismic sequential ground motions are input along the weak axis direction of the structural cross section (i.e., the X direction) respectively. Thus, the first and sixth natural frequencies have a large contribution to the response, which corresponds to the predominant period of ground motion 1.397s and 0.328s.

Focusing on the analysis of ground motions spectral characteristics, in Fig. 13, several typical seismic sequential ground motions were selected on each site class. Elastic response spectra of mainshocks and the corresponding aftershocks were calculated respectively, to compare the difference of spectral characteristics between them. An identical damping ratio of 0.05 was used. The controlling periods of both the intact structure and damaged structure are shown in Fig. 13. Existing studies [37–40] and Fig. 13 show that the spectral components of ground motions vary widely depending on the condition of site class. The softer the site, the more low-frequency components tend to be found in the ground motion, i.e., the predominant period of ground motion increases. In the meantime, the high-rise building had a longer natural vibration period compared with the ordinary multi-story building, which caused the structural response to be more susceptible to long-periodic components of ground motion. Therefore, in the selected ground motions recorded on site class A, response spectra were small near the natural vibration period, coincident with low level structural responses. In the selected ground motions recorded on site class D, mainshock response spectra have abundant long-periodic components, especially at the first natural period of 1.397s. When mainshocks are applied, structural damage is much more severe and reaches the level of serious damage. Because the response spectra of corresponding aftershocks on site class D were smaller than the mainshock near the first natural period of the structure, structural damage indexes were not significantly increased. This is consistent with the structural damage indexes obtained by nonlinear time history analysis shown in Figs. 9 and 12.

For seismic sequential ground motions with large increases in structural damage indexes (i.e., the ground motion in Figs. 10 and 11), two typical ground motions were selected for each site class.

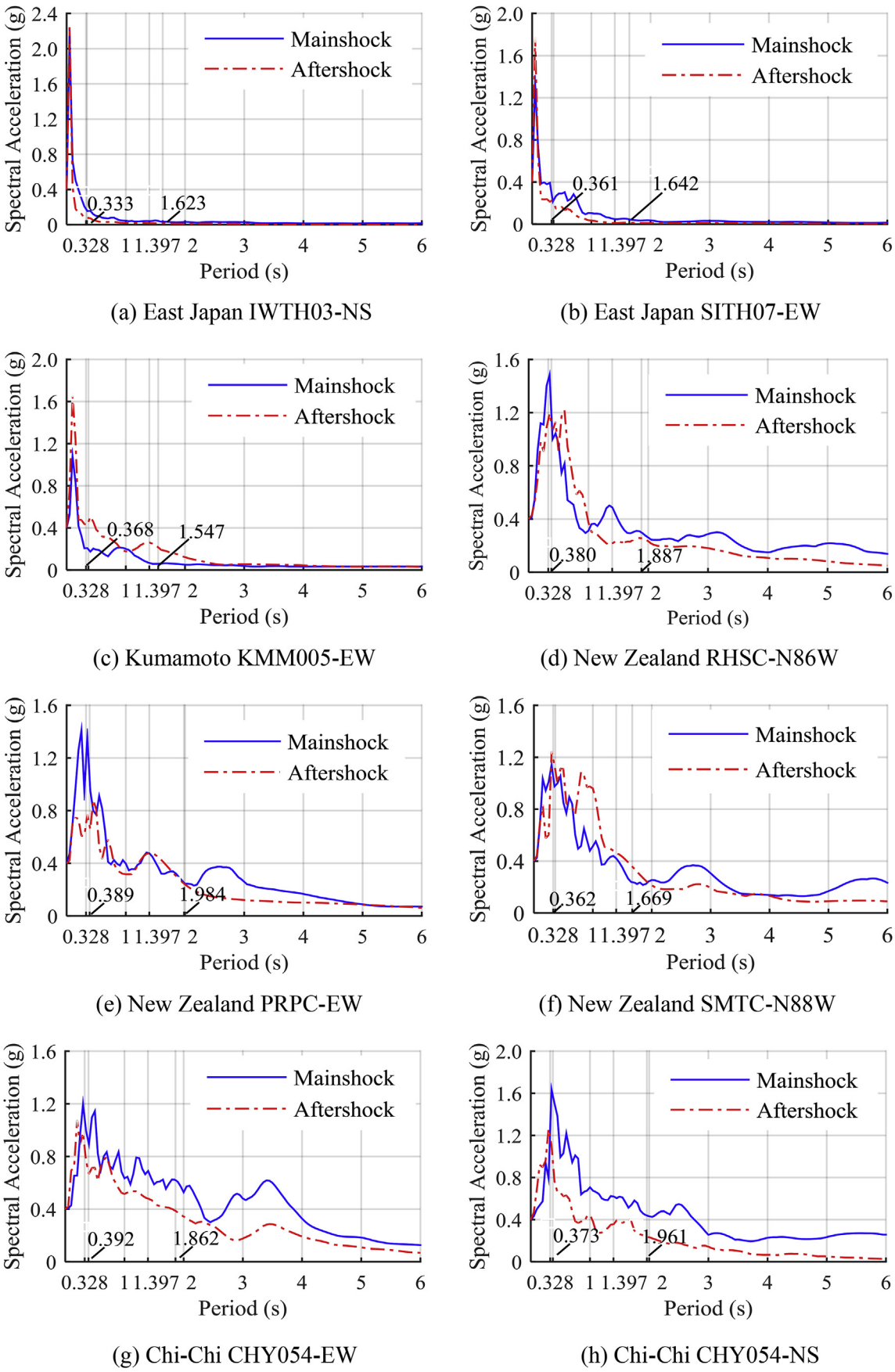

Fig. 13. Comparison of response spectra of main shock and corresponding aftershocks. (a, b) Site class A, (c, d) Site class B, (e, f) Site class C, and (g, h) Site class D.

Mainshocks and aftershocks in the elastic response spectra were calculated separately, and the results are shown in Fig. 13(c–f). Damping ratio is equal to 0.05. The comparisons show that for the same seismic sequential ground motions, the frequency components of the mainshock and aftershock are quite different. The aftershock may have larger spectral accelerations than the mainshock, especially around natural periods, such as in Fig. 13 (c). On the other hand, in the natural vibration period of the structure, the spectrum value of the mainshock is generally larger than the aftershock, which means if the sequential ground motion is simulated by repeating mainshock, the damage of the structure may be overestimated [18]. Therefore, under the excitation of aftershocks, structural displacement responses and hysteretic energy consumption levels have increased. Correspondingly, structural damage indexes experienced a large increase, which tends to makes the structural performance level unsafe.

As noted from the experimental results shown thus far, the spectral characteristics of mainshocks and aftershocks in seismic sequential ground motions are significantly different. In the structural analysis, the artificially induced ground motion cannot be simply used to simulate the seismic sequential ground motion by repeating the mainshock motion or by randomly composing ground motions. The as-recorded seismic sequential ground motions should be used for studying structural response. Moreover, the influence of seismic sequential ground motions on a structure is mainly controlled by the frequency (period) distribution of the mainshock and aftershock. Therefore, even if the frame-core tube structure incurs no significant damage under the mainshock, there is still the possibility of serious damage under the excitation of aftershocks. That is, the effects of aftershocks cannot be ignored. The serious damage is more likely to occur on sites where the soil is softer, and the ground motion has a large amplitude for long-periodic components. Aftershocks should be considered when designing the high-rise building. In addition, the structure has the possibility of serious damage under the mainshock on site class D. It is recommended to consider the sensitivity of the structural response to the long-periodic component of the ground motion when constructing high-rise buildings on soft soil foundations. Due to the small number of selected ground motions recorded in site class D experiment, the influence of aftershocks in the selected small samples is not significant. The response of the frame-core tube structure subjected to seismic sequential ground motions on site class D needs further study.

6. Conclusions

The authors collected 104 as-recorded seismic sequential ground motions for four different site classes. With the superior computing power of the Tianhe-2 supercomputer, the nonlinear time-history analysis method was used for the frame-core tube structure subjected to mainshocks and sequence-type ground motions separately. Then, the damage indexes of the structure are given based on the Park-Ang damage model. Meanwhile, the structural performance level is quantitatively evaluated. Finally, combined with the response spectrum of the mainshock and aftershock, the conclusions of the structural study are as follows:

(1) Using a supercomputer, typical finite element calculation analysis problems can be efficiently solved in the field of structural engineering. In this research, for the frame-core tube structure, using only a small number of Tianhe-2 compute nodes can improve the computational efficiency by 140 times compared with the common PC. Its excellent computational stability is suitable for large-scale parallel computation. Researchers are advised to consider high-performance supercomputers for calculations when doing large-scale structural analysis to save computation time.
(2) Inclusion of aftershocks leads to a longer duration than mainshock, which has a greater impact on the cumulative hysteresis energy. Thus, the possibility of structural damage is increased. On the other hand, the spectral characteristics of seismic sequential mainshock-aftershock tested site events were significantly different. This was especially true in the softer areas of the sites and in the long-periodic components of the aftershock, which corresponds to the natural period of the structure. Thus, the long-periodic nature of the aftershocks has a possibility of inflicting structural damages several times larger than the mainshock. Therefore, in the design of high-rise buildings, the possibility of aftershock secondary damages on a structure or even multiple damages to a structure cannot be ignored.
(3) The reinforced concrete cylinder of the frame-core tube structure has a good effect in resisting the lateral load by the mainshock, and the structural damage condition is basically maintained within the repairable range. However, for the softer area of the site, the frame-core tube structure located above it has the possibility of a large increase in the damage index when the aftershocks come. The corresponding performance level can change from a repairable state to a severe damage or even collapse status. Therefore, for the softer area of a site, the anti-collapse design of high-rise buildings also needs to consider the effects of aftershocks.

In fact, for high-rise buildings, there are many factors that affect their structural safety, such as strong winds and fires. In order to emphasize the influence of seismic sequential ground motion on the frame-core tube structure, this paper only considers the impact of a single disaster on the test structure. It should be noted that future research will consider the impact of multiple hazards and carry on a more comprehensive study of high-rise buildings.

Acknowledgments

The authors would like to acknowledge the financial support provided by National Natural Science Foundation of China (U1711264).

Appendix A. Supplementary data

Supplementary data to this article can be found online at https://doi.org/10.1016/j.soildyn.2019.05.036.

References

[1] Tsai KC, Hsiao CP, Bruneau M. Overview of building damages in 921 Chi-Chi earthquake. Earthq Eng Eng Seismol 2000;2:93–108.
[2] Wang Z. A preliminary report on the great wenchuan earthquake. Earthq Eng Eng Vib 2008;7:225–34.
[3] Moon L, Dizhur D, Senaldi I, Derakhshan H, Griffith M, Magenes G, et al. The demise of the URM building stock in Christchurch during the 2010–2011 Canterbury earthquake sequence. Earthq Spectra 2014;30:253–76.
[4] Kazama M, Noda T. Damage statistics (summary of the 2011 off the pacific coast of Tohoku earthquake damage). Soils Found 2012;52:780–92.
[5] Chen H, Xie Q, Li Z, Xue W, Liu K. Seismic damage to structures in the 2015 Nepal earthquake sequences. J Earthq Eng 2017;21:551–78.
[6] Daniell J, Vervaeck A. Damaging earthquakes database 2011-the year in review Available online at https://www.cedim.kit.edu/.
[7] Omori F. On the aftershocks of earthquake. J Coll Sci Imp Univ Tokyo, Japan 1895;7.
[8] Gutenberg B, Richter CF. Seismicity in the Earth and associated phenomena n.d. 1954.
[9] Bath M. Lateral inhomogeneities of the upper mantle. Tectonophysics 1965;2:483–514.
[10] Mahin SA. Effects of duration and aftershocks on inelastic design earthquakes. Proc. 7th world Conf. Earthq. Eng. 1980;5:677–80.
[11] Ruiz-García J, Moreno JY, Maldonado IA. Evaluation of existing Mexican highway bridges under mainshock-aftershock seismic sequences. 14 th world conf. Earthq. Eng. 2008.
[12] Zhai CH, Wen WP, Chen Z, Li S, Xie LL. Damage spectra for the mainshock–-aftershock sequence-type ground motions. Soil Dynam Earthq Eng 2013;45:1–12.
[13] Zhang Y, Chen J, Sun C. Damage-based strength reduction factor for nonlinear structures subjected to sequence-type ground motions. Soil Dynam Earthq Eng 2017;92:298–311.
[14] Raghunandan M, Liel AB, Luco N. Aftershock collapse vulnerability assessment of reinforced concrete frame structures. Earthq Eng Struct Dyn 2015;44:419–39.
[15] Hatzigeorgiou GD, Beskos DE. Inelastic displacement ratios for SDOF structures

subjected to repeated earthquakes. Eng Struct 2009;31:2744–55.
[16] Hatzigeorgiou GD, Liolios AA. Nonlinear behaviour of RC frames under repeated strong ground motions. Soil Dynam Earthq Eng 2010;30:1010–25.
[17] Council on tall buildings and urban habitat. 2008 Available at http://www.ctbuh.org/.
[18] Ruiz-García J, Negrete-Manriquez JC. Evaluation of drift demands in existing steel frames under as-recorded far-field and near-fault mainshock–aftershock seismic sequences. Eng Struct 2011;33:621–34.
[19] Amadio C, Fragiacomo M, Rajgelj S. The effects of repeated earthquake ground motions on the non-linear response of SDOF systems. Earthq Eng Struct Dyn 2003;32:291–308.
[20] Vafaee MH, Saffari H. A modal shear-based pushover procedure for estimating the seismic demands of tall building structures. Soil Dynam Earthq Eng 2017;92:95–108.
[21] Lu Z, Chen X, Lu X, Yang Z. Shaking table test and numerical simulation of an RC frame-core tube structure for earthquake-induced collapse. Earthq Eng Struct Dyn 2016;45:1537–56.
[22] Lu X, Xie L, Guan H, Huang Y, Lu X. A shear wall element for nonlinear seismic analysis of super-tall buildings using OpenSees. Finite Elem Anal Des 2015;98:14–25.
[23] Miao ZW, Lu XZ, Jiang JJ, Ye LP. Nonlinear FE model for RC shear walls based on multi-layer shell element and microplane constitutive model. Comput Methods Eng Sci EPMESC X 2006:405–11.
[24] Hellesland J, Scordelis A. Analysis of RC bridge columns under imposed deformations. IABSE Colloq; 1981. p. 545–59.
[25] Spacone E, Filippou FC, Taucer FF. Fibre beam–column model for non-linear analysis of R/C frames: Part I. Formulation. Earthq Eng Struct Dyn 1996;25:711–25.
[26] Reddy JN. Mechanics of laminated composite plates and shells: theory and analysis. CRC press; 2004.
[27] PEER ground motion database. 2018 Available online at http://ngawest2.berkeley.edu/.
[28] Kyoshin-Net. National research institute for earth science and disaster prevention. 2018 Available at http://www.k-net.bosai.go.jp/.
[29] Guo F, WU D, XU G, JI Y. Site classification corresponding relationship between Chinese and the overseas seismic design codes [J]. J Civ Eng Manag 2011;2:12.
[30] GB50011 CS. Code for seismic design of buildings. China Build Ind Press Beijing; 2010.
[31] Recode. 2015 Available online at https://www.recode.net/2015/7/13/11614652/.
[32] National supercomputer center in guangzhou. 2018 Available online at www.nscc-gz.cn/Product/.
[33] Chung RM. January 17, 1995 Hyogoken-Nanbu (Kobe) earthquake: performance of structures, lifelines, and fire protection systems (NIST SP 901). 1996.
[34] Park Y-J, Ang AH-S. Mechanistic seismic damage model for reinforced concrete. J Struct Eng 1985;111:722–39.
[35] Park YJ, Ang AH-S, Wen YK. Seismic damage analysis of reinforced concrete buildings. J Struct Eng 1985;111:740–57.
[36] Kunnath SK, Reinhorn AM, Park YJ. Analytical modeling of inelastic seismic response of R/C structures. J Struct Eng 1990;116:996–1017.
[37] Ding Y, Peng Y, Li J. Cluster Analysis of earthquake ground-motion records and characteristic period of seismic response spectrum. J Earthq Eng 2018;1–22.
[38] Seed HB, Ugas C, Lysmer J. Site-dependent spectra for earthquake-resistant design. Bull Seismol Soc Am 1976;66:221–43.
[39] Sabetta F, Pugliese A. Estimation of response spectra and simulation of nonstationary earthquake ground motions. Bull Seismol Soc Am 1996;86:337–52.
[40] Akinci A, Malagnini L, Sabetta F. Characteristics of the strong ground motions from the 6 April 2009 L'Aquila earthquake, Italy. Soil Dynam Earthq Eng 2010;30:320–35.